Journal of NAMP 73 (2026) 21-45

The Nigerian Association of Mathematical Physics

Journal homepage: https://nampjournals.org.ng

ANALYTICAL AND THERMODYNAMIC STUDY OF DIATOMIC MOLECULES IN A COMPOSITE QUANTUM INTERACTION POTENTIAL

Etido P. Inyang[*1], Jonathan E. Osang[2], Christopher C. Ekechukwu[3], Oyelami O. Abiodun[4], Olumuyiwa O. Akintola[5], Eddy S. William[6]

[1]Department of Physics, Faculty of Science, National Open University of Nigeria, Jabi-Abuja, Nigeria, [2]Department of Physics, University of Cross River State, Calabar, [3]Department of Physics, University of Calabar, Calabar, Nigeria, [4]Department of Mathematics, Faculty of Science, National Open University of Nigeria, Jabi-Abuja, Nigeria, [5]Department of Chemistry, Faculty of Science, National Open University of Nigeria, Jabi-Abuja, Nigeria and [6]Department of Physics, School of Pure and Applied Sciences, Federal University of Technology, Ikot Abasi, Nigeria

Corresponding Authors e-mail: einyang@noun.edu.ng

ARTICLE INFO

Article history:
Received xxxxx
Revised xxxxx
Accepted xxxxx
Available online xxxxx

Keywords:
Modified Kratzer potential,
generalized inverse quadratic Yukawa potential,
Schrödinger equation,
Exact quantization rule
Formula method

Abstract

In this research, we obtained the energy eigenvalues and the corresponding normalized eigenfunctions for a linear combination of the modified Kratzer and generalized inverse quadratic Yukawa potentials using two analytical approaches: the exact quantization rule and the formula method. Furthermore, we evaluated the thermodynamic properties, including the ro-vibrational mean energy, ro-vibrational free energy, ro-vibrational entropy, and ro-vibrational specific heat capacity. Numerical results were computed for selected diatomic molecules, namely N_2, CO, NO, and CH, and were found to be in good agreement with existing results reported in the literature. In addition, graphical analyses were carried out to investigate the behavior of the energy spectrum associated with the proposed potential.

1. Introduction

The study of the thermodynamic properties and energy spectra of diatomic molecules plays a crucial role in understanding molecular behavior and interactions at different temperature conditions. Through the investigation of molecular energy spectra, the vibrational and rotational states of molecules

[*]Corresponding author: Etido P. Inyang
E-mail address: einyang@noun.edu.ng
https://doi.org/10.60787/jnamp.vol73no.726

can be determined, thereby providing insight into important thermodynamic quantities such as entropy, internal energy, free energy, and specific heat capacity. In quantum mechanics, the eigen wave function, which describes the probability distribution of particles in a quantum system, is obtained by solving the Schrödinger equation (SE) under a given potential in the non-relativistic regime [1–5]. Notably, the eigenfunction contains all the necessary information required for a complete description of the quantum system at any instant of time [6]. Consequently, considerable attention has been devoted to developing efficient techniques for obtaining exact or approximate solutions of the Schrödinger equation due to the mathematical complexities associated with the equation. These complexities mainly arise from the centrifugal term encountered during the separation of the wave equation in spherical coordinates [7]. Over the years, several analytical and approximation methods have been proposed to address these challenges. Among these are the Nikiforov–Uvarov (NU) method [8–12], the asymptotic iteration method (AIM) [13], the Nikiforov–Uvarov functional analysis (NUFA) method [14–16], the series expansion method [17–20], and the Wentzel–Kramers–Brillouin (WKB) approximation [21–23], among others [24,25]. Despite these developments, obtaining exact analytical solutions for realistic and complex potential models in one-dimensional (1D), three-dimensional (3D), or even idealized systems such as the Coulomb, harmonic oscillator, and Kratzer potentials remains a challenging task [26,27]. This challenge has continued to stimulate research interest in the search for more accurate, efficient, and experimentally consistent solution techniques. As a result, the development of improved potential models and analytical approaches has remained an active area of research in both relativistic and non-relativistic quantum mechanics [14–25]. One promising approach involves the linear combination or superposition of different potential models. This technique imposes stronger constraints on the particle motion, thereby improving the flexibility and applicability of the resulting model in describing physical systems [28,29]. In the present work, we employ the exact quantization rule (EQR) approach and the formula method to obtain approximate analytical solutions of the radial Schrödinger equation for arbitrary quantum numbers in D-dimensional space. The system under consideration involves a particle interacting through a linear combination of the modified Kratzer potential and the generalized inverse quadratic Yukawa potential [30–33].To validate the effectiveness of the proposed approach, our results are compared with those reported using other established analytical methods. The modified Kratzer potential [34] has attracted significant attention in quantum chemistry, molecular physics, and atomic physics because of its effectiveness in describing molecular interactions [35]. The potential consists of an attractive long-range term and a short-range repulsive term, making it highly suitable for describing both rotational and vibrational energy spectra of diatomic molecules [36,37]. The modified Kratzer potential is given by:

$$V_{MKP}\left(r\right) = D_e\left(\frac{r - r_e}{r}\right)^2 \tag{1a}$$

where D_e is the dissociation energy and r_e is the equilibrium inter-molecular distance and r the inter-molecular distance. Its attributes are such that $V_{MKP}\left(r\right) \to \infty$ when $r \to 0$ and vice versa [38].

On the other hand, the generalized inverse quadratic Yukawa potential (GIQYP) was first introduced by Ikhdair *et al.* [39]. This potential represents a linear combination of the inverse quadratic Yukawa potential [40] and the conventional Yukawa potential [41]. The Yukawa potential plays a significant role in atomic and molecular physics as a screened Coulomb potential used to describe the distribution of electronic charge clouds surrounding the nucleus [42]. Furthermore, in particle physics, it is widely employed to model short-range interactions between hadrons within gauge theories through the exchange of massive scalar mesons [43]. One key attribute of the GIQYP is that

it approaches a finite value $r \to \infty$ and $V_{GIQYP}(r) \to \infty$ as $r \to 0$ as making it particularly useful for specific applications. It is of the form

$$V_{GIQYP}(r) = -V\left(1 - \frac{e^{-\delta r}}{r}\right)^2 \tag{1b}$$

where V is the potential coupling strength and δ is the screening parameter or the potential range. The motivation for considering a linear combination of the modified Kratzer potential and the generalized inverse quadratic Yukawa potential arises from the need to describe both the long-range and short-range characteristics of molecular interactions within a single framework. The modified Kratzer potential has been widely employed in molecular spectroscopy because it accurately models the vibrational and rotational motion of diatomic molecules through its dependence on the equilibrium bond length and dissociation energy. However, the potential primarily describes the molecular bonding region and may not adequately account for screening effects and short-range interactions present in realistic molecular environments.

In contrast, the generalized inverse quadratic Yukawa potential incorporates a screening parameter that effectively characterizes short-range interactions resulting from electronic charge distributions and shielding effects. Such interactions are particularly important in molecular and atomic systems where deviations from pure Coulombic behavior occur due to the presence of surrounding electron clouds.

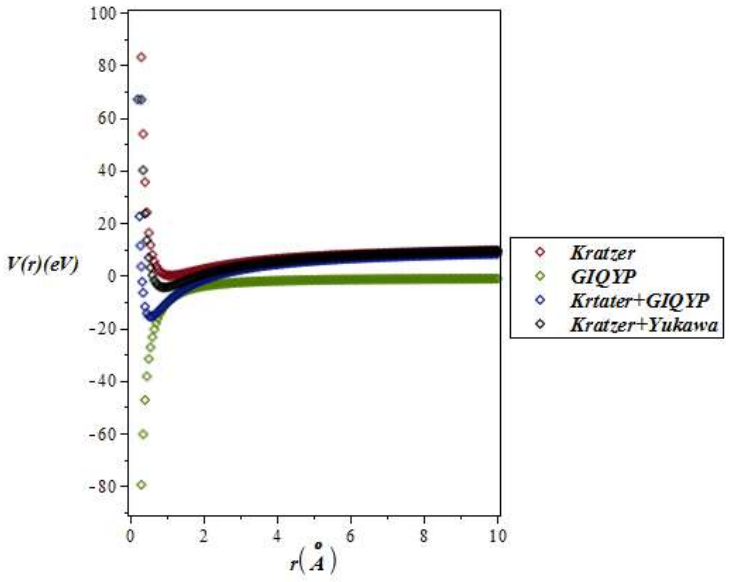

FIG. 1 Spectral comparison of four molecular potential

By superposing these two potentials, the resulting model combines the strengths of both constituent interactions. The modified Kratzer component provides an accurate description of the bound ro-vibrational states of diatomic molecules, while the GIQYP contribution introduces additional flexibility through screening and inverse quadratic terms that account for short-range corrections. Consequently, the combined potential is expected to offer a more realistic representation of molecular interactions than either potential alone, particularly for diatomic systems where both bonding characteristics and screened interactions influence the energy spectrum and thermodynamic properties. This enhanced flexibility is also reflected in the deeper potential well exhibited by the

proposed potential compared with the individual constituent potentials, as shown in Figure 1, indicating stronger confinement and improved suitability for molecular spectroscopy studies.+
Combining Eqs. (1a) and (1b), we obtain the potential under investigation as

$$V(r) = D_0 - \frac{D_1}{r} + \frac{D_2}{r^2} - D_3 - \frac{D_4 e^{-\delta r}}{r} - \frac{D_5 e^{-2\delta r}}{r^2} \tag{1c}$$

where $D_0 = D_e,\ D_1 = 2D_e r_e,\ D_2 = D_e r_e^2,\ D_3 = D_5 = V$ and $D_4 = 2V$

Figure 1 presents a comparative plot of the proposed potential with three related potentials, namely the modified Kratzer potential, the Kratzer plus Yukawa potential, and the generalized inverse quadratic Yukawa potential (GIQYP). The proposed potential exhibits a deeper potential well, indicating its greater suitability and effectiveness in describing diatomic molecular systems in molecular spectroscopy. Several studies have been carried out on both the constituent potentials and their linear combinations with other interaction potentials using different analytical approaches. For example, Edet *et al.* [44] obtained the eigensolutions of the non-central generalized inverse quadratic Yukawa potential using the Nikiforov–Uvarov (NU) method. In another study, Edet *et al.* [45] investigated the energy- spectra of N_2, CO, NO, and CH diatomic molecules interacting through a linear combination of the modified Kratzer and Yukawa potentials within the framework of the NU method. Oluwadare and Oyewumi [46] derived the energy eigenvalues and corresponding eigenfunctions of the Schrödinger equation with the GIQYP using the proper quantization rule approach. Furthermore,Inyang [47] examined the influence of the q-deformation parameter on the eigenstates of the information thoery via the NU method. Similarly, Obu *et al.* [48] obtained the relativistic and non-relativistic energy eigenvalues together with their corresponding eigenfunctions for a linear combination of the Hulthén and Kratzer potentials using the NU approach. Inyang *et al.* [49] studied the bound state solutions of the Schrödinger equation with the inverse quadratic Yukawa potential using the NU method. Berkdemir *et al.* [50] derived the non-relativistic energy eigenvalues and corresponding eigenfunctions of the Kratzer potential and applied the model to investigate the energy states of H_2, N_2, O_2, and CO diatomic molecules. In another related work, Inyang *et al.* [51] solved the Klein–Gordon equation with the Eckart–Hellmann potential model using the NU method and obtained analytical expressions for the ro-vibrational energy spectra. Their study included the numerical computation of bound state energies for different screening parameters and quantum states, as well as the ro-vibrational energies of VH, TiH, NiC, TiC, and CuLi diatomic molecules. Moreover, Bayray *et al.* [52] employed the asymptotic iteration method (AIM) to derive the exact energy eigenvalues and the associated eigenfunctions of related quantum systems. The remainder of this paper is organized as follows: Section 2 presents a brief review of the exact quantization rule approach. In Section 3, the method is applied to obtain the bound state solutions of the modified Kratzer plus generalized inverse quadratic Yukawa potential. Section 4 discusses some special cases of the potential obtained through appropriate parameter adjustments. In Section 5, the thermodynamic properties of the system are evaluated. Section 6 presents the results and discussion, while the concluding remarks are provided in Section 7.

2.0 Review of Exact quantization rule approach

The exact quantization rule (EQR) [30] is an improved form of the Wentzel–Kramers–Brillouin (WKB) approximation [22], which incorporates an additional integral term($N\pi$) known as the quantum correction term Q_c. This correction term remains constant for exactly solvable potentials and is independent of the number of nodes of the wave function. In the following sections, we briefly demonstrate how the energy eigenvalues of all bound states of a quantum system can be conveniently

determined using the exact quantization rule. In addition, we show how the ground-state solution can be obtained through the solution of the Riccati equation [53].

The one-dimensional Schrödinger equation is given by

$$\frac{d^2\psi(x)}{dx^2} = -\frac{2\mu}{\hbar^2}\left[E - V(x)\right]\psi(x), \tag{2}$$

where $V(x)$ is the piecewise continuous real potential function of x satisfying the following conditions:

$$\begin{aligned} &V(x) < E, \quad && x_a < x < x_b, \\ &V(x) = E \quad && x_a = x \quad \text{or} \quad x = x_b, \\ &V(x) > E \quad && x \in (-\infty, x_a) \text{ or } x \in (x_b, \infty), \end{aligned} \tag{3}$$

where x_a and x_b are two turning points determined by $E - V(x) = 0$.

In the form of a non-linear Ricatti equation, equation (2) can be written as:

$$\frac{d}{dx}\phi(x) = -\frac{2\mu}{\hbar^2}\left[E - V(x)\right]\psi(x) - \phi(x)^2 \tag{4}$$

where $\phi(x) = \psi(x)^{-1}\, d\psi(x)/dx$ is the logarithmic derivative of the wave function $\psi(x)$; for the non-relativistic Schrödinger equation, $\phi(x)$ represents the phase angle of the wave function. The Ricatti equation as given by equation (4) reveals that for $E \geq V(x)$, as the variable x increases across the nodes of the wave function $\psi(x)$, the logarithmic derivative decreases to $-\infty$, jumps to $+\infty$, and then, decreases again.

As proposed and studied by Ma and Xu [32], the exact quantization rule for the one-dimensional Schrödinger equation is given by

$$\begin{aligned} &\int_{x_a}^{x_b} k_n(x)\,dx = (n+1)\pi + \int_{x_a}^{x_b} \phi(x)\left[\frac{dk_n(x)}{dx}\right]\left[\frac{d\phi(x)}{dx}\right]^{-1} dx \\ &\text{and} \quad k_n(x) = \sqrt{\frac{2\mu}{\hbar^2}}\left[E - V_{eff}(x)\right]^{\frac{1}{2}} \qquad E \geq V_{eff}(x), \end{aligned} \tag{5}$$

where again, x_a and x_b are the two turning points obtained by solving the quadratic equation posed by $E - V_{eff}(r) = 0$.

The first term $(n+1)$ represents the classical contribution associated with the nodes $\phi(x)$, of the wave function, while the second term Q_c, is the quantum correction term that accounts for quantum effects arising from the logarithmic derivative of the wave function. This correction is responsible for the improved accuracy of the EQR over the conventional WKB approximation, so that the ground state quantum correction Q_{c0} can be calculated as

$$Q_{c0} = \int_{x_a}^{x_b} \phi_0(x)\left[\frac{dk_0(x)}{dr}\right]\left[\frac{d\phi_0(r)}{dr}\right]^{-1} dx. \tag{6}$$

The quantum correction term is typically evaluated using standard integration tables. However, when the resulting integrand is not available in the literature, it can be computed using software packages such as Maple, Python, or similar tools.

In extending this method to the three-dimensional Schrödinger equation with a central potential, the radial part of the Schrödinger equation becomes:

$$\frac{d^2R(r)}{dr^2} = -\frac{2\mu}{\hbar^2}\left[E - V_{eff}\left(r\right)\right]R\left(r\right), \qquad V_{eff}\left(r\right) = V(r) + \frac{\hbar^2 l(l+1)}{2\mu r^2}. \tag{7}$$

By comparing equations (2) and (7), the energy eigenvalues of the Schrödinger equation can be calculated by matching the conditions of the logarithmic derivatives. In this context, the logarithmic derivative is defined as: $\phi(r) = [dR/dr]/R(r)$. By applying this approach, we can see that, from the quantization rule (equation (5)), the energy eigenvalues of the three-dimensional Schrödinger equation are given by:

$$\int_{r_a}^{r_b} k_n\left(r\right)dr = (n+1)\pi + \int_{r_a}^{r_b}\phi\left(r\right)\left[\frac{dk\left(r\right)}{dr}\right]\left[\frac{d\phi\left(r\right)}{dr}\right]^{-1}dr \qquad k_n\left(r\right) = \sqrt{\frac{2\mu}{\hbar^2}}\left[E - V_{eff}\left(r\right)\right]^{\frac{1}{2}} \qquad E \geq V_{eff}\left(r\right), \tag{8}$$

where r_a and r_b are the two turning points obtained by solving the quadratic equation posed by $E = V_{eff}\left(r\right)$.

3.0 Application of the exact quantization rule to Kratzer plus GIQYP potential

In this section, we will demonstrate how to apply the exact quantization rule technique to calculate the energy spectra of the Schrödinger equation (SE) with the Kratzer plus GIQYP potential. The SE with an interaction potential in D-dimensions [54] is given by:

$$-\frac{\hbar^2}{2\mu}\nabla_D^2\psi\left(r,\Omega_D\right) + \left[E - V\left(r\right)\right]\psi\left(r,\Omega_D\right) = 0 \tag{9}$$

where D is the dimensionality and $D \geq 2$; $\hbar$ and μ are the reduced Planck constant and mass respectively; ∇_D^2 is the Laplacian in D-dimensions; E is the non-relativistic energy and the wave function is expressed as $\psi\left(r,\Omega_D\right) = r^{-\frac{D-1}{2}}R_{nl}\left(r\right)Y_{lm}\left(\Omega_D\right)$ and $Y_{lm}\left(\Omega_D\right)$ is the generalized spherical harmonic function. The eigenvalues of the angular momentum operator L_D^2 for this function is $L_D^2 Y_{lm}\left(\Omega_D\right) = l\left(l + D - 2\right)Y_{lm}\left(\Omega_D\right)$.

From the foregoing, (see Appendix A) the radial Schrödinger equation with the combined potential can be written as:

$$\frac{d^2R_{nl}\left(r\right)}{dr^2} + \frac{2\mu}{\hbar^2}\left[E_{nl} - \left\{D_0 - \frac{D_1}{r} + \frac{D_2}{r^2} - D_3 - \frac{D_4 e^{-\delta r}}{r} - \frac{D_5 e^{-2\delta r}}{r^2} + \frac{K\left(K+1\right)\hbar^2}{2\mu r^2}\right\}\right]R_{nl}\left(r\right) = 0 \tag{10}$$

where $K = l + \frac{1}{2}\left(D-3\right)$; n and l are the principal and orbital angular momentum quantum numbers respectively; r is the inter-nuclear distance. For the short-range potential considered in this study, the Greene and Aldrich approximation scheme [55] is employed to overcome the difficulty associated with the centrifugal barrier term in Equation (10). This approximation simplifies the radial

Schrödinger equation by providing an appropriate treatment of the centrifugal term, thereby enabling the radial part of the equation to be expressed as follows: $\frac{1}{r^2} \approx \frac{\delta^2 e^{2\delta r}}{\left(e^{\delta r}-1\right)^2}$. (11)

Using equation (11), the Schrödinger equation in equation (10) becomes:

$$\frac{d^2R_{nl}(r)}{dr^2}+\frac{2\mu}{\hbar^2}\left[E_{nl}-\left\{\begin{matrix} D_0-\frac{D_1\delta}{\left(1-e^{-\alpha r}\right)}+\frac{D_2\delta^2}{\left(1-e^{-\alpha r}\right)^2} \\ -D_3-\frac{D_4\delta e^{-\delta r}}{\left(1-e^{-\alpha r}\right)}-\frac{D_5\delta^2e^{-2\delta r}}{\left(1-e^{-\alpha r}\right)^2}+\frac{K(K+1)\hbar^2\delta^2}{2\mu r^2\left(1-e^{-\alpha r}\right)^2}\end{matrix}\right\}\right]R_{nl}(r)=0. \quad (12)$$

The term in curly brackets in equation (12) is the effective potential $V_{eff}(r)$, containing the combine potential and the centrifugal barrier. That is,

$$V_{eff}(r)=D_0-\frac{D_1\delta}{\left(1-e^{-\delta r}\right)}+\frac{D_2\delta^2}{\left(1-e^{-\delta r}\right)^2}-D_3-\frac{D_4\delta e^{-\delta r}}{\left(1-e^{-\delta r}\right)}-\frac{D_5\delta^2e^{-2\delta r}}{\left(1-e^{-\delta r}\right)^2}+\frac{K(K+1)\hbar^2\delta^2}{2\mu r^2\left(1-e^{-\delta r}\right)^2} \quad (13)$$

$$=D_0-\frac{D_1\delta e^{\delta r}}{\left(e^{\delta r}-1\right)}+\frac{D_2\delta^2e^{2\delta r}}{\left(e^{\delta r}-1\right)^2}-D_3-\frac{D_4\delta}{\left(e^{\delta r}-1\right)}-\frac{D_5\delta^2}{\left(e^{\delta r}-1\right)^2}+\frac{K(K+1)\hbar^2\delta^2e^{2\delta r}}{2\mu\left(e^{\delta r}-1\right)^2}$$

Using the coordinate transformation, $x=\frac{1}{e^{\delta r}-1}$, we will have $e^{\delta r}=\frac{1+x}{x}$, so that

$$V_{eff}(x)=D_0-D_1\delta(1+x)+D_2\delta^2(1+x)^2-D_3-D_4\delta x-D_4\delta^2x^2+\frac{K(K+1)\hbar^2\delta^2}{2\mu}(1+x)^2. \quad (14)$$

Factorizing the above expression in terms of x, we obtain

$$V_{eff}(x)=\left(D_0-D_1\delta+D_2\delta^2-D_3+\frac{K(K+1)\hbar^2\delta^2}{2\mu}\right)$$

$$+\left(-D_1\delta+2D_2\delta^2-D_4\delta+\frac{2K(K+1)\hbar^2\delta^2}{2\mu}\right)x+\left(D_2\delta^2-D_5\delta^2+\frac{K(K+1)\hbar^2\delta^2}{2\mu}\right)x^2 \quad (15)$$

$$D_0-D_1\delta(1+x)+D_2\delta^2(1+x)^2-D_3-D_4\delta x-D_4\delta^2x^2+\frac{K(K+1)\hbar^2\delta^2}{2\mu}(1+x)^2$$

The two turning points x_a and x_b which are determined by solving $V(x)=E_{nl}$ quadratically are given as

$$x_a=-\frac{G}{2C}-\frac{\sqrt{G^2-4C(H-E_{nl})}}{2C}, \quad (16)$$

$$x_b=-\frac{G}{2C}+\frac{\sqrt{G^2-4C(H-E_{nl})}}{2C}, \quad (17)$$

where

$$\left\{\begin{array}{l} H = D_0 - D_1\delta + D_2\delta^2 - D_3 + \dfrac{K(K+1)\hbar^2\delta^2}{2\mu}, \\ G = -D_1\delta + 2D_2\delta^2 - D_4\delta + \dfrac{2K(K+1)\hbar^2\delta^2}{2\mu}, \\ \text{and} \\ C = D_2\delta^2 - D_5\delta^2 + \dfrac{K(K+1)\hbar^2\delta^2}{2\mu} \end{array}\right\}. \tag{18}$$

The momentum between the two turning points x_a and x_b is

$$k(x) = \sqrt{\frac{2\mu}{\hbar^2}}\left[E_{nl} - V_{eff}(x)\right]^{\frac{1}{2}} \tag{19}$$

By substituting equation (18) into equation (15) and making use of the two properties of turning points, that is, $x_a + x_b = -\dfrac{G}{C}$ and $x_a x_b = \dfrac{H - E_{nl}}{C}$, we obtain

$$k(x) = \sqrt{\frac{2\mu C}{\hbar^2}}\left[(-1)(x_a - x)(x - x_b)\right]^{\frac{1}{2}} \tag{20}$$

In terms of the variable τ, the non-linear Ricatti equation for the ground state becomes

$$-\delta x(1+x)\frac{d}{dx}\phi_0(x) + \phi_0^2(x) + \frac{2\mu}{\hbar^2}\left[E_{0\ell} - V_{eff}(x)\right]\phi_0(x) = 0. \tag{21}$$

From its monotonic property, the logarithmic derivative of $\phi_0(x)$ for the ground state has one node and no pole, therefore, we assume a trial solution of the form $\phi_0(x) = A + Bx$. Upon substituting this into equation (21), and evaluating, we obtain the following expression:

$$A^2 + (2AB - \delta B)x + (B^2 - \delta B)x^2 = \frac{2\mu}{\hbar^2}\left[H - E_{0l} + Gx - Cx^2\right] \tag{22}$$

Upon comparing the LHS and RHS of equation (22), we obtain

$$\left\{\begin{array}{l} A^2 = \dfrac{2\mu}{\hbar^2}(H - E_{0\ell}) \\ B = \dfrac{\delta}{2} \pm \dfrac{1}{2}\sqrt{\delta^2 + \dfrac{8\mu C}{\hbar^2}} \end{array}\right\} \tag{23}$$

The above problem is physically solvable for only B since here, the logarithmic derivative of $\phi_0(x)$ will decrease exponentially as physically required.

From the foregoing, the integral of the momentum $k(r)$ (i.e. LHS of eq. (8)) for $n = 0$ is evaluated as follows:

$$\begin{aligned} \int_{r_a}^{r_b} k_0(r)\,dr &= -\int_{x_a}^{x_b} k(x)\frac{dx}{\delta x(1+x)} = -\frac{1}{\delta}\sqrt{\frac{2\mu C}{\hbar^2}}\int_{x_a}^{x_b}\frac{\sqrt{(-1)(x-x_a)(x-x_b)}}{x(1+x)}dx \\ &= -\frac{\pi}{\delta}\sqrt{\frac{2\mu C}{\hbar^2}}\left[\sqrt{(x_a+1)(x_b+1)} - 1 - \sqrt{x_a x_b}\right] \\ &= -\frac{\pi}{\delta}\sqrt{\frac{2\mu C}{\hbar^2}}\left[\sqrt{\frac{H - E_{nl} - G + C}{C}} - 1 - \sqrt{\frac{H - E_{nl}}{C}}\right] \end{aligned}, \tag{24}$$

and the ground state quantum correction Q_{c0} (which can be generalized to any value of $\eth$), is

$$Q_{c0} = \int_{r_a}^{r_b} \phi_0(r)\left[\frac{dk_0(r)}{dr}\right]\left[\frac{d\phi_0(r)}{dr}\right]^{-1} dr = -\int_{x_a}^{x_b} \frac{\phi_0(x)}{\delta x(1+x)}\left[\frac{dk_0(x)}{dx}\right]\left[\frac{d\phi_0(x)}{dx}\right]^{-1} dx$$

$$= \frac{1}{\delta}\sqrt{\frac{2\mu C}{\hbar^2}}\int_{x_a}^{x_b} \frac{\left(x-\frac{x_a+x_b}{2}\right)\left(x+\frac{A}{B}\right)}{x(1+x)\sqrt{(-1)(x-x_a)(x-x_b)}}dx.$$

$$= \frac{1}{\delta}\sqrt{\frac{2\mu C}{\hbar^2}}\int_{x_a}^{x_b} \frac{\left[\left(\frac{A}{B}-1\right)\left(1+\frac{x_a+x_b}{2}\right)x-\frac{A}{B}\left(\frac{x_a+x_b}{2}\right)(1+x)+x(1+x)\right]}{x(1+x)\sqrt{(-1)(x-x_a)(x-x_b)}}dx$$

$$= \frac{\pi}{\delta}\sqrt{\frac{2\mu C}{\hbar^2}}\left[\frac{\left(\frac{A}{B}-1\right)\left(1+\frac{x_a+x_b}{2}\right)}{\sqrt{(x_a+1)(x_b+1)}}-\frac{\frac{A}{B}\left(\frac{x_a+x_b}{2}\right)}{\sqrt{x_a x_b}}+1\right]$$

$$= \frac{\pi}{\delta}\sqrt{\frac{2\mu C}{\hbar^2}}\left[\frac{1}{B}\frac{\sqrt{2\mu C}}{\hbar}+1\right]$$

evaluated as $= \pi\left(\frac{B}{\delta}-1+\frac{1}{\delta}\frac{\sqrt{2\mu C}}{\hbar}\right)$ (25)

Noting that for all exactly solvable quantum systems, the quantum correction Q_c is independent of the number of nodes $\eth$ of the wavefunction, we can put equation (24) and equation (25), in equation (8). Doing so, equation (8) becomes

$$-\frac{\pi}{\delta}\sqrt{\frac{2\mu C}{\hbar^2}}\left[\sqrt{\frac{H-E_{nl}-G+C}{C}}-\sqrt{\frac{H-E_{nl}}{C}}-1\right] = (n+1)\pi+\pi\left(\frac{B}{\delta}-1+\frac{1}{\delta}\frac{\sqrt{2\mu C}}{\hbar}\right). \quad (26)$$

From the above expression, the energy spectra E_{nl} is thus given explicitly as

$$E_{nl} = D_0 - D_1\delta + D_2\delta^2 - D_3 + \frac{K(K+1)\hbar^2\delta^2}{2\mu} -$$

$$\frac{\hbar^2}{8\mu}\left[\frac{\frac{2\mu}{\hbar^2}\left(D_1\delta - D_2\delta^2 + D_4\delta - D_5\delta^2 - \frac{K(K+1)\hbar^2\delta^2}{2\mu}\right)}{(B+\alpha n)} - (B+\alpha n)\right]^2 \quad (27)$$

where $B = \frac{\alpha}{2}+\sqrt{\frac{\delta^2}{4}+\frac{2\mu C}{\hbar^2}}$ (28)

It is important to note that one of the major limitations of the exact quantization rule approach is its inability to provide explicit expressions for the wave functions of quantum systems. To overcome this limitation, we employ the formula method developed in Ref. [56] (see Appendix C) to obtain the corresponding wave functions for the potential considered in this study. By applying this method to Equation (12), the following parameters are obtained:

$k_4 = \sqrt{\varepsilon-\sigma_1}$, (29)

$$k_5 = G, \tag{30}$$

Thus, in terms of Jacobi polynomials, the resulting wave function for the Kratzer plus GIQYP for $s = e^{-\delta r}$ is given as

$$R(s) = N_{nl} e^{\sqrt{\varepsilon-\sigma_1}} (1-s)^G \, {}_2F_1\left(-n, n+2\left(\sqrt{\varepsilon-\sigma_1}+G\right); 2\sqrt{\varepsilon-\sigma_1}+1, s\right), \tag{31}$$

where $G = \frac{1}{2} + \sqrt{\frac{1}{4} + 4\varepsilon - \sigma_4 - \sigma_2}$, $\varepsilon = -\frac{2\mu}{\hbar^2}\left(E_{nl} - D_0 + D_3\right)$, $\sigma_1 = \frac{2\mu D_1}{\hbar^2}$,

$\sigma_2 = -\frac{2\mu D_1}{\hbar^2} + K(K+1)$, $\sigma_3 = \frac{2\mu D_4}{\hbar^2}$, and $\sigma_4 = \frac{2\mu D_5}{\hbar^2}$

And from the definition of Jacobi polynomials [57]

$$P_n^{(\theta,\varphi)}(x) = \frac{\Gamma(n+\theta+1)}{n!\Gamma(\theta+1)} \, {}_2F_1\left(-n, \theta+\varphi+n+1, \theta+1; \frac{1-x}{2}\right) \tag{32}$$

$$R(s) = N_{nl} e^{\sqrt{\varepsilon-\sigma_1}} (1-s)^G \, P_n^{\left(2\sqrt{\varepsilon-\sigma_1}, 2G-1\right)}(1-2s), \tag{33}$$

where N_{nl} is the normalization constant and it is obtained as follows;

$$\int_0^\infty \left|R_{nl}(r)\right|^2 dr = 1 \tag{34}$$

$$-\int_1^0 \left|R_{nl}(s)\right|^2 \frac{ds}{\delta s} = 1 \tag{35}$$

Changing the variable as $y = 1-2s$, and then, $\frac{1-y}{2} = s$ and $\frac{1+y}{2} = 1-s$, eq. (35) becomes

$$\frac{N^2}{2\delta}\int_{-1}^{1}\left(\frac{1-y}{2}\right)^{2A-1}\left(\frac{1+y}{2}\right)^{2G}\left[P_n^{(2A,2G-1)}(y)\right]^2 dy = 1 \tag{36}$$

And $A = \sqrt{\varepsilon-\sigma_1}$

Noting that $\frac{N^2}{2\delta}\int_{-1}^{1}\left(\frac{1-y}{2}\right)^{a}\left(\frac{1+y}{2}\right)^{b}\left[P_n^{(a,b)}(y)\right]^2 dy = \frac{2\Gamma(a+n+1)\Gamma(b+n+1)}{n!a\Gamma(a+b+n+1)}$ (37)

Hence, our normalization constant becomes

$$N = \sqrt{\frac{2\delta n!(2A-1)\Gamma(2A+2G+n)}{2\Gamma(2A+n)\Gamma(2G+n+1)}} \tag{38}$$

4.0 Limiting cases of the energy eigenvalues spectrum

By making appropriate adjustments to some of the constants in equation (1c), we obtain the limiting cases of the energy eigenvalues given by equation (27). These limiting cases are in excellent agreement with known results in the literature, validating the correctness of our approach for: $D = 3$, and $K \to l$. Doing this we realized the following six limiting cases:

a. Kratzer potential

Setting $D_3 = D_4 = D_5 = 0$ in equation (1c), it reduces to the Kratzer potential (KP),

$$V_{MKP}(r) = D_0 - \frac{D_1}{r} + \frac{D_2}{r^2}, \tag{39}$$

and the expression for energy eigenvalues from equation (27) taking that $\delta \to 0$ becomes

$$\cdot E_{nl} = D_0 - \frac{2\mu D_1^2}{\hbar^2\left(n+\frac{1}{2}+\sqrt{\frac{1}{4}+\frac{2\mu D_2}{\hbar^2}+l\left(l+1\right)}\right)^2} \tag{40}$$

The above equation represents the energy eigenvalue expression for the Kratzer potential (KP), which is identical to equation (14) reported in reference [58].

b. GIQYP potential

Setting $D_0 = D_1 = D_2 = 0$ in equation (1c), it reduces to the GIQYP potential,

$$V_{GIQYP}\left(r\right) = -D_3 - \frac{D_4 e^{-\delta r}}{r} - \frac{D_5 e^{-2\delta r}}{r^2}, \tag{41}$$

and the expression for energy eigenvalues from equation (27) becomes

$$E_{nl} = -D_3 + \frac{l\left(l+1\right)\hbar^2\delta^2}{2\mu} -$$

$$\frac{\hbar^2}{8\mu}\left[\frac{\frac{2\mu}{\hbar^2}\left(D_4 - D_5\delta - \frac{l\left(l+1\right)\hbar^2\delta}{2\mu}\right)}{\left(n+\frac{1}{2}+\sqrt{\frac{1}{4}-\frac{2\mu D_5}{\hbar^2}+l\left(l+1\right)}\right)} - \delta\left(n+\frac{1}{2}+\sqrt{\frac{1}{4}-\frac{2\mu D_5}{\hbar^2}+l\left(l+1\right)}\right)\right]^2 \tag{42}$$

The above equation represents the energy eigenvalue expression for the GIQYP, which is identical to the result reported in reference [44].

c. IQYP potential

Setting $D_0 = D_1 = D_2 = D_3 = D_4 = 0$ in equation (1c), it reduces to the IQYP potential,

$$V_{IQYP}\left(r\right) = -\frac{D_5 e^{-2\delta r}}{r^2}, \tag{43}$$

and the expression for energy eigenvalues from equation (27) becomes

$$E_{nl} = \frac{l\left(l+1\right)\hbar^2\delta^2}{2\mu} -$$

$$\frac{\hbar^2}{8\mu}\left[\frac{\frac{2\mu}{\hbar^2}\left(-D_5\delta - \frac{l\left(l+1\right)\hbar^2\delta}{2\mu}\right)}{\left(n+\frac{1}{2}+\sqrt{\frac{1}{4}-\frac{2\mu D_5}{\hbar^2}+l\left(l+1\right)}\right)} - \delta\left(n+\frac{1}{2}+\sqrt{\frac{1}{4}-\frac{2\mu D_5}{\hbar^2}+l\left(l+1\right)}\right)\right]^2 \tag{44}$$

d. Yukawa potential

Setting $D_0 = D_1 = D_2 = D_3 = D_5 = 0$ in equation (1c), it reduces to the Yukawa potential (YP),

$$V_{IQYP}\left(r\right) = -\frac{D_4 e^{-\delta r}}{r}, \tag{45}$$

and the expression for energy eigenvalues from equation (27) becomes

$$E_{nl} = \frac{l(l+1)\hbar^2\delta^2}{2\mu} -$$

$$\frac{\hbar^2}{8\mu}\left[\frac{\frac{2\mu}{\hbar^2}\left(D_4 - \frac{l(l+1)\hbar^2\delta}{2\mu}\right)}{\left(n+\frac{1}{2}+\sqrt{\frac{1}{4}+l(l+1)}\right)} - \delta\left(n+\frac{1}{2}+\sqrt{\frac{1}{4}+l(l+1)}\right)\right]^2 \quad (46)$$

The above equation represents the energy eigenvalue expression for the Yukawa potential (YP), which is identical to the results reported in reference [59].

e. Hellmann potential

Setting $D_0 = D_2 = D_3 = D_5 = 0$ and $D_4 \to -D_4$ in equation (1c), it reduces to the Hellmann potential (HP),

$$V_{IQYP}(r) = -\frac{D_1}{r} + \frac{D_4 e^{-\delta r}}{r}, \quad (47)$$

and the expression for energy eigenvalues from equation (27) becomes

$$E_{nl} = -D_1\delta + \frac{l(l+1)\hbar^2\delta^2}{2\mu} -$$

$$\frac{\hbar^2}{8\mu}\left[\frac{\frac{2\mu}{\hbar^2}\left(D_1 + D_4 - \frac{l(l+1)\hbar^2\delta}{2\mu}\right)}{\left(n+\frac{1}{2}+\sqrt{\frac{1}{4}+l(l+1)}\right)} - \delta\left(n+\frac{1}{2}+\sqrt{\frac{1}{4}+l(l+1)}\right)\right]^2 \quad (48)$$

The energy eigenvalue of the Hulthén potential (HP) is identical to the results reported in reference [60].

f. Coulomb potential

Setting $D_0 = D_2 = D_3 = D_4 = D_5 = 0$ in equation (1c), it reduces to the Coulomb potential,

$$V_{IQYP}(r) = -\frac{D_1}{r}, \quad (49)$$

and the expression for energy eigenvalues from equation (27) taking that $\delta \to 0$ becomes

$$E_{nl} = -\frac{2\mu D_1^2}{\hbar^2(n+l+1)^2}. \quad (50)$$

The energy eigenvalue of the Coulomb potential is identical to the results reported in reference [61].

5.0 Thermodynamic properties of the modified Kratzer plus GIQYP potential

The ro-vibrational partition function for a bound state system of any diatomic molecules (DMs) at temperature T, as given in references [62, 63], is expressed as:

$$z_{vib}(\beta) = \sum_{n=0}^{\lambda} e^{-\beta E_{nl}}, \beta = (kT)^{-1} \quad (51)$$

where λ is the upper bound vibrational quantum number, k is the Boltzmann's constant, β is the fluctuation parameter and the ro-vibrational energy eigenvalues of the modified Kratzer plus GIQYP is given as E_{nl}. The derivation of the partition function in Eq. (51) relies on the continuum (or

classical) approximation, in which the discrete summation over quantum states is replaced by an integral. This approximation is justified when the thermal energy+ is sufficiently large compared with the spacing between adjacent energy levels, such that many bound states contribute to the partition function. Under these conditions, the energy spectrum may be treated as quasi-continuous, leading to a computationally tractable expression for the thermodynamic quantities. Consequently, the present thermodynamic analysis is expected to be most accurate in the moderate- and high-temperature regimes, whereas deviations may occur at very low temperatures where the discrete nature of the quantum energy spectrum becomes significant.

Substituting eq. (27) into eq. (51), yields

$$z(\beta)=\sum_{v=0}^{\lambda} e^{-\beta\left[P_1-\frac{\hbar^2}{8\mu}\left(\frac{P_2}{(B+\delta n)}-(B+\delta n)\right)^2\right]} \tag{52}$$

where $P_1=D_0-D_1\delta+D_2\delta^2-D_3+\dfrac{K(K+1)\hbar^2\delta^2}{2\mu}$,

$P_2=D_1\delta-D_2\delta^2+D_4\delta-D_5\delta^2-\dfrac{K(K+1)\hbar^2\delta^2}{2\mu}$.

Replacing the sum by an integral in the classical limit, we obtain

$$z(\beta)=\int_0^{\lambda} e^{\left[\beta L\rho^2+\frac{M\beta}{\rho^2}+N\beta\right]}d\rho,\quad \rho=B+\delta n \tag{53}$$

where $L=\dfrac{\hbar^2}{8\mu}$, $M=\dfrac{\hbar^2P_2^2}{8\mu}$, and $N=-P_1-\dfrac{2\hbar^2P_2}{8\mu}$ (54)

Employing a Maple software to evaluate the ro-vibrational partition function, we obtain

$$z(\beta)=\frac{1}{2}e^{\left(L\beta\rho^2+N\beta\right)}\sqrt{M\beta}\left(\frac{2\lambda e^{\frac{M\beta}{\lambda^2}}}{\sqrt{M\beta}}-\frac{2\sqrt{M\beta\pi}\,erfi\left(\frac{\sqrt{M\beta}}{\lambda}\right)}{\sqrt{M\beta}}-2\sqrt{\pi}\right) \tag{55}$$

And the imaginary error function is defined by ref. [63] as

$$erfi(y)=\frac{erf(iy)}{i}=\frac{2}{\sqrt{\pi}}\int_0^{y}e^{x^2}dx \tag{56}$$

The following thermodynamic properties of the modified Kratzer plus GIQYP potential are obtained using the ro-vibrational partition function from equation (51):

Ro-vibrational mean energy:

$$U(\beta)=-\frac{\partial\ln z(\beta)}{\partial\beta}=-\frac{1}{2z(\beta)}\left[2z(\beta)\left(L\rho^2+N\right)+\frac{z(\beta)}{2\sqrt{M\beta}}+W(\beta)\right] \tag{57}$$

where $W(\beta)=\dfrac{1}{2}e^{\left(L\beta\rho^2+N\beta\right)}\sqrt{M\beta}\left(-\dfrac{\lambda e^{\frac{M\beta}{\lambda^2}}M}{(M\beta)^{3/2}}-\dfrac{\sqrt{M\pi}\,erfi\left(\frac{\sqrt{M\beta}}{\lambda}\right)}{\sqrt{M\beta^2}}-\dfrac{M^{3/2}\sqrt{\beta\pi}\,erfi\left(\frac{\sqrt{M\beta}}{\lambda}\right)}{(M\beta)^{3/2}}\right)$ (58)

Ro-vibrational free energy:

$$F(\beta)=\frac{\ln z(\beta)}{\beta} \tag{59}$$

Ro-vibrational entropy:

$$\begin{aligned} S(\beta) &= k\ln z(\beta)-k\beta\frac{\partial \ln z(\beta)}{\partial\beta} \\ &= k\ln z(\beta)-\frac{k\beta}{2z(\beta)}\left[\left[2z(\beta)\left(L\rho^2+N\right)+\frac{z(\beta)}{2\sqrt{M\beta}}+W(\beta)\right]\right] \end{aligned} \tag{60}$$

Ro-vibrational specific heat capacity

$$C_v(\beta)=k\beta^2\frac{\partial^2 \ln z(\beta)}{\partial\beta^2}$$

$$= k\beta^2\left[\begin{array}{l} \frac{1}{2z(\beta)}\left[\begin{array}{l} 2z(\beta)\left(L\rho^2+N\right)^2+\frac{z(\beta)M}{\sqrt{M\beta}}\left(L\rho^2+N\right)+2W(\beta)\left(L\rho^2+N\right) \\ -\frac{z(\beta)M^2}{4(M\beta)^{3/2}}+W(\beta)M+T(\beta) \end{array}\right] \\ -\frac{1}{2z(\beta)}\left[2z(\beta)\left(L\rho^2+N\right)+\frac{z(\beta)M}{2\sqrt{M\beta}}+W(\beta)\left(L\rho^2+N\right)\right] \\ -\frac{1}{2z(\beta)M\beta}\left[z(\beta)\left(L\rho^2+N\right)+\frac{z(\beta)M}{2\sqrt{M\beta}}+W(\beta)\right]M \\ -\frac{1}{2z(\beta)}\left[2z(\beta)\left(L\rho^2+N\right)+\frac{z(\beta)M}{2\sqrt{M\beta}}+W(\beta)\right]2e^{-L\rho^2-N\beta}W(\beta) \end{array}\right] \tag{61}$$

where

$$T(\beta)=\frac{1}{2}e^{\left(L\beta\rho^2+N\beta\right)}\sqrt{M\beta}\left(\begin{array}{l} -\frac{3\lambda e^{\frac{M\beta}{\lambda^2}}M^2}{2(M\beta)^{5/2}}+\frac{\sqrt{M\pi}erfi\left(\frac{\sqrt{M\beta}}{\lambda}\right)}{2\sqrt{M\beta}\beta^{3/2}}- \\ \frac{e^{\frac{M\beta}{\lambda^2}}M}{\lambda\beta\sqrt{M\beta}}+\frac{M^{3/2}\sqrt{\beta\pi}erfi\left(\frac{\sqrt{M\beta}}{\lambda}\right)}{\sqrt{\beta}(M\beta)^{3/2}}-\frac{3M^{5/2}\sqrt{\beta\pi}erfi\left(\frac{\sqrt{M\beta}}{\lambda}\right)}{2(M\beta)^{5/2}} \end{array}\right) \tag{62}$$

6.0 Results and discussion

In theoretical, computational, experimental, and quantum chemical investigations, the relationships between physical observables are commonly established by examining how relevant quantities respond to variations in system parameters. Such analyses are typically carried out through numerical computations and graphical representations, which provide valuable insight into the underlying physical behavior of the system. In the present work, Equation (27) was employed to generate the numerical results reported in the tables and figures, thereby facilitating a detailed analysis of the energy spectrum and thermodynamic properties of the system. The spectroscopic parameters of the selected diatomic molecules were obtained from Ref. [45].

The accuracy and reliability of the Exact Quantization Rule (EQR) method are assessed in Tables 1–4 through comparisons with previously reported results for the Yukawa and modified Kratzer potentials at different values of the principal quantum number, (n), and angular momentum quantum number, (l). As shown in Tables 1 and 2, the present EQR results for the Yukawa potential are in excellent agreement with those obtained using the Nikiforov–Uvarov (NU) method and other available numerical data, confirming the validity of the approach. Similarly, Tables 3 and 4 present comparisons for the modified Kratzer potential applied to the diatomic molecules N_2, CO, NO, and CH. The close agreement between the present results and those reported in the literature further demonstrates the robustness and accuracy of the EQR formalism.

Table 5 presents the calculated energy eigenvalues for the proposed linear combination of the modified Kratzer and generalized inverse quadratic Yukawa potentials for the same set of diatomic molecules. The results provide insight into the influence of the composite potential on bound-state systems. It is observed that the energy eigenvalues increase with increasing values of both (n) and (l). Physically, larger values of (n) correspond to higher excited states, while increasing (l) enhances the centrifugal contribution to the effective potential, resulting in an overall increase in the energy spectrum. This behavior is consistent with the expected characteristics of quantum bound states.

The thermodynamic properties derived from the partition function further elucidate the thermal behavior of the molecular systems. The ro-vibrational mean energy increases with temperature for all molecules considered, reflecting the progressive population of higher vibrational and rotational states as thermal energy increases. This trend is consistent with the Boltzmann distribution, according to which an increasing number of accessible energy levels contributes to the total internal energy of the system.

In contrast, the ro-vibrational free energy decreases with increasing temperature due to the growing contribution of entropy, which lowers the free energy and enhances the thermodynamic stability of the system. Molecules characterized by larger energy level separations generally exhibit more pronounced variations in free energy than those possessing closely spaced levels.

The ro-vibrational entropy is found to increase monotonically with temperature. At low temperatures, only a limited number of quantum states are occupied, resulting in relatively low disorder. As the temperature rises, additional rotational and vibrational states become thermally accessible, leading to a greater degree of randomness and a corresponding increase in entropy.

Similarly, the ro-vibrational specific heat capacity increases rapidly at lower temperatures before gradually approaching a nearly constant value at higher temperatures. This behavior reflects the progressive activation of rotational and vibrational degrees of freedom. Once a substantial fraction of the available states becomes populated, further increases in temperature produce comparatively smaller changes in the energy storage capacity of the molecules.

A comparison among N_2, CO, NO, and CH reveals that the magnitude and temperature dependence of the thermodynamic quantities are strongly influenced by molecular spectroscopic parameters, particularly the reduced mass, dissociation energy, and equilibrium bond length. Molecules with larger dissociation energies generally possess more tightly bound states and therefore exhibit lower thermal excitation at a given temperature. Conversely, molecules with smaller dissociation energies respond more readily to thermal fluctuations. These findings demonstrate that the combined modified Kratzer–GIQYP potential effectively captures the thermal characteristics of diatomic molecular systems and provides a reliable framework for investigating their thermodynamic behavior over a broad temperature range.

To further explore the influence of potential parameters on the energy spectrum, graphical analyses were performed. Figure 2 illustrates the dependence of the energy eigenvalues on the screening parameter for different quantum states. The results show that the energy spectrum decreases

exponentially as the screening parameter increases, indicating that stronger screening weakens the effective interaction and lowers the bound-state energies.

Figures 3 and 4 depict the variation of the energy spectrum with respect to the dissociation energy and equilibrium bond length, respectively. In both cases, the energy eigenvalues increase with increasing parameter values. However, Figure 4 reveals that the energy levels corresponding to different quantum states gradually converge at larger equilibrium bond lengths, suggesting a reduced sensitivity of the spectrum to quantum state variations in this regime.

Figure 5 presents the dependence of the energy spectrum on the coupling strength associated with the generalized inverse quadratic Yukawa component of the potential. An exponential decay behavior is observed, with the energy eigenvalues decreasing and approaching zero as the coupling strength increases. This trend indicates that stronger coupling significantly modifies the effective interaction, thereby reducing the energy of the bound states.

Table 1 Energy eigenvalue of the Yukawa potential for $D_4 = \sqrt{2}\ eV,\ \delta = 2gD_4\ \mathring{A}^{-1}$ and $\hbar = \mu = 1$

n	g	Our work	[64]	[65]	[66]	[67]
1s	0.002	-0.99600400	-0.99600	0.99600	0.99601	0.99600
	0.005	-0.99002500	-0.99002	-0.99003	-0.99004	-0.99000
	0.01	-0.98010000	-0.98010	-0.98014	-0.98015	-0.98010
	0.02	-0.96040000	-0.96040	-0.96059	-0.96059	-0.96060
	0.025	-0.95062500	-0.95062	-0.95092	-0.95092	-0.95090
	0.05	-0.90250000	-0.90250	-0.90363	-0.90363	-0.90360
2s	0.002	-0.24601600	-0.24601	-0.24602	-0.24602	-0.24600
	0.005	-0.24010000	-0.24010	-0.24014	-0.24015	-0.24010
	0.01	-0.23040000	-0.23040	-0.23058	-0.23059	-0.23060
	0.02	-0.21160000	-0.21160	-0.21229	-0.21230	-0.21230
	0.025	-0.20250000	-0.20250	-0.20355	-0.20355	-0.20360
	0.05	-0.16000000	-0.16000	-0.16354	-0.16351	-0.16350
3p	0.002	-0.10714711	-0.10714	-0.10716	-0.10716	-0.10720
	0.005	-0.10133611	-0.10133	-10.10141	-0.10142	-0.10140
	0.01	-0.09201111	-0.09201	-0.09230	-0.09231	-0.09231
	0.02	-0.07471111	-0.07471	-0.07570	-0.07570	-0.07570
	0.025	-0.06673611	-0.06673	-0.06815	-0.06814	-0.06816
	0.05	-0.03361111	-0.03361	-0.03711	-0.03739	-0.03712

Table 2: Energy eigenvalue (fm^{-1}) of the Yukawa potential for $\delta = 0.4\ \mathring{A}^{-1}$ and $\hbar = 2\mu = 1$

n	l	V	Our work	[64]	[65]	[66]	[67]
0	0	4	-3.2400	-3.2400	-3.2564	-3.2563	-3.2565
0	0	8	-14.4400	-14.4400	-14.4581	-14.4581	-14.4571
0	0	16	-60.8400	-60.8400	-60.8590	-60.8590	-60.8590
1	0		-12.9600	-12.9600	-13.0273	-13.0270	-13.0273
2	0		-4.2711	-4.2711	-4.3941	-4.3937	-4.3720
0	0	24	-139.2400	-139.2400	-139.2593	-139.2590	-139.2594
1	0		-31.3600	-31.3600	-31.4312	-31.4310	31.4356
2	0		-11.5600	-11.5600	-11.6998	-11.6990	-11.6998
3	0		-4.8400	-4.8400	-5.0441	-5.0448	-5.0442
4	0		-1.9600	-1.9600	-2.2033	-2.2194	-2.2033

Table 3 Energy eigenvalues (eV) of the modified Kratzer potential for N_2 and CO diatomic molecules

n	l	N_2	N_2 [45]	N_2 [50]	CO	CO [45]	CO [50]
0	0	0.054440080	0.054433681	0.054430000	0.052255280	0.050829440	0.050823000
1	0	0.162087030	0.162077140	0.162057000	0.151304950	0.151304930	0.151287000
	1	0.162331330	0.162565720	0.162546000	0.151539300	0.151773620	0.151755000
2	0	0.268278120	0.268261600	0.268229000	0.250384090	0.250384040	0.250354000
	1	0.268519110	0.268743590	0.268711000	0.250615190	0.250846240	0.250160000
	2	0.268760110	0.269707440	0.269675000	0.250846280	0.251770530	0.251744000
3	0	0.373039460	0.373016320	0.372972000	0.348092620	0.348092540	0.348051000
	1	0.373277220	0.373491830	0.373447000	0.348320530	0.348548350	0.348507000
	2	0.373514980	0.374442740	0.374398000	0.348548430	0.349459880	0.349418000
	3	0.373752710	0.375868810	0.375823000	0.348776330	0.350826870	0.350785000
4	0	0.476396630	0.476366850	0.476313000	0.444455700	0.444455580	0.444403000
	1	0.476631210	0.476836010	0.476779000	0.444680480	0.444905140	0.444852000
	2	0.476865780	0.477774200	0.477717000	0.444905260	0.445804140	0.445751000
	3	0.477100340	0.479181190	0.479124000	0.445130020	0.447152360	0.447099000
	4	0.477334900	0.481056650	0.480999000	0.445354770	0.448949420	0.448895000
5	0	0.578374590	0.578338180	0.578269000	0.539497920	0.539497750	0.539434000
	1	0.578606050	0.578801090	0.578732000	0.539719630	0.539941160	0.539877000
	2	0.578837500	0.579726790	0.579658000	0.539941330	0.540827870	0.540764000
	3	0.579068940	0.581115060	0.581046000	0.540163030	0.542157650	0.542093000
	4	0.579300380	0.582965540	0.582896000	0.540384700	0.543930150	0.543865000
	5	0.579531790	0.585277800	0.585208000	0.540606380	0.546144910	0.546082000

Table 4: Energy eigenvalues (eV) of the modified Kratzer potential for NO and CH diatomic molecules

n	l	NO	NO [45]	NO [50]	CH CH [45]	CH [50]	
0	0	0.041123182	0.041123195	0.041118000	0.083229281	0.083224184	0.083214000
1	0	0.122325847	0.122325849	0.122311000	0.241166826	0.241151503	0.241123000
	1	0.122532363	0.122738863	0.122724000	0.242796715	0.244409838	0.244381000
2	0	0.202298811	0.202298791	0.202274000	0.389616956	0.389591425	0.389547000
	1	0.202502208	0.202705567	0.202681000	0.391149930	0.392656024	0.392611000
	2	0.202705589	0.203518990	0.203494000	0.392681567	0.398769202	0.398722000
3	0	0.281066784	0.281066733	0.281033000	0.529324618	0.529288943	0.529229000
	1	0.281267123	0.281467399	0.281434000	0.530768211	0.532174862	0.532115000
	2	0.281467447	0.282268597	0.282235000	0.532210564	0.537931848	0.537870000
	3	0.281667764	0.283470085	0.283436000	0.533651675	0.546530346	0.546467000
4	0	0.358653849	0.358653765	0.358611000	0.660963052	0.660917327	0.660844000
	1	0.358851193	0.359048434	0.359006000	0.662324079	0.663638196	0.663565000
	2	0.359048521	0.359837651	0.359795000	0.663683954	0.669066127	0.668992000
	3	0.359245841	0.361021173	0.360997800	0.665042676	0.677173658	0.677098000
	4	0.359443146	0.362598630	0.362555000	0.666400248	0.687920044	0.687842000
5	0	0.435083496	0.435083367	0.435032000	0.785141917	0.785086272	0.785001000
	1	0.435277902	0.435472163	0.435421000	0.786426557	0.787654439	0.787569000
	2	0.435472295	0.436249637	0.436198000	0.787710125	0.792777921	0.792692000
	3	0.435666677	0.437415549	0.437364000	0.788992619	0.800431163	0.800343000
	4	0.435861048	0.438969538	0.438917000	0.790274044	0.810576230	0.810487000
	5	0.436055409	0.440911128	0.440858000	0.791554398	0.823163305	0.823071000

Table 5 Energy eigenvalues (eV) of the modified Kratzer plus generalized inverse quadratic potential for N_2, CO, NO and CH diatomic molecules

n	l	N_2	CO	NO	CH
0	0	0.142352681	0.079536704	0.014314254	-0.015022938
1	0	0.231091461	0.161726684	0.077928111	0.087074134
	1	0.231298580	0.161924070	0.078093559	0.088113175
2	0	0.318667994	0.242811630	0.140618894	0.183536394
	1	0.318872465	0.243006426	0.140781998	0.184520073
	2	0.319076937	0.243201199	0.140945119	0.185503039
3	0	0.405102462	0.322811236	0.202404332	0.274770012
	1	0.405304331	0.323003481	0.202565139	0.275702240
	2	0.405506198	0.323195709	0.202725961	0.276633802
	3	0.405708049	0.323387955	0.202886761	0.277564692
4	0	0.490414609	0.401744741	0.263301746	0.361145198
	1	0.490613911	0.401934494	0.263460301	0.362029544
	2	0.490813220	0.402124225	0.263618873	0.362913262
	3	0.491012513	0.402313965	0.263777424	0.363796353
	4	0.491211784	0.402503688	0.263935964	0.364678821
5	0	0.574623738	0.479630988	0.323328038	0.442999946
	1	0.574820524	0.479818282	0.323484388	0.443839670
	2	0.575017318	0.480005559	0.323640739	0.444678804
	3	0.575214097	0.480192846	0.323797087	0.445517353
	4	0.575410853	0.480380105	0.323953415	0.446355317
	5	0.575607626	0.480567359	0.324109740	0.447192694

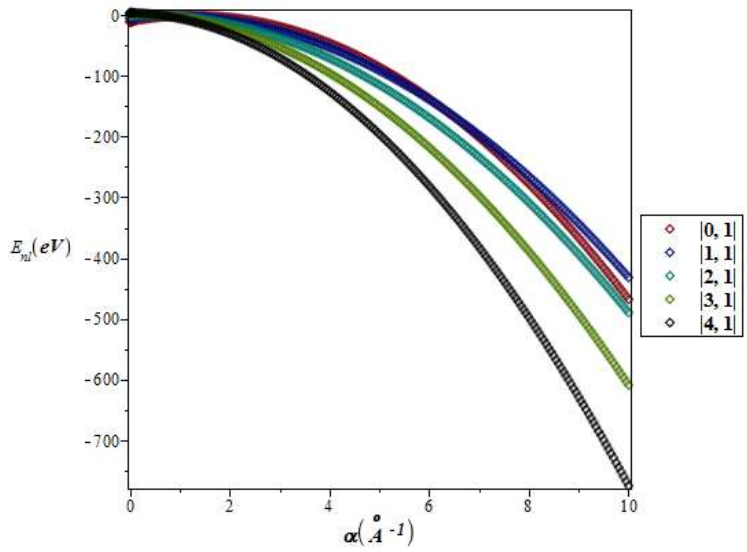

FIG. 2 Plot of energy eigenvalue spectrum against potential range

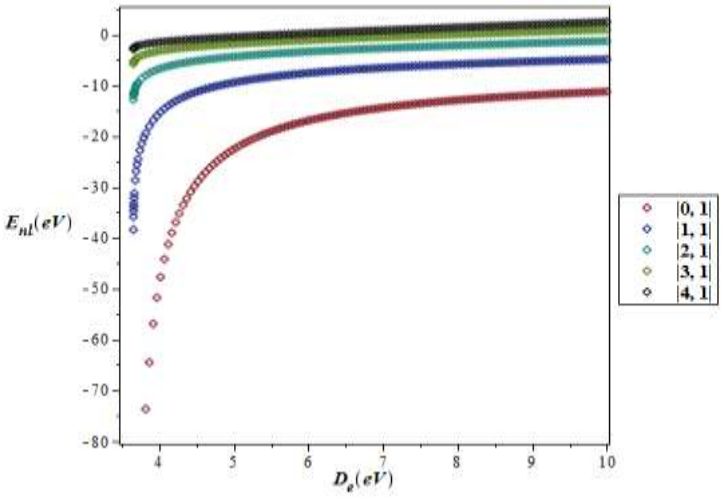

FIG. 3 Plot of energy eigenvalue spectrum against Dissociation energy

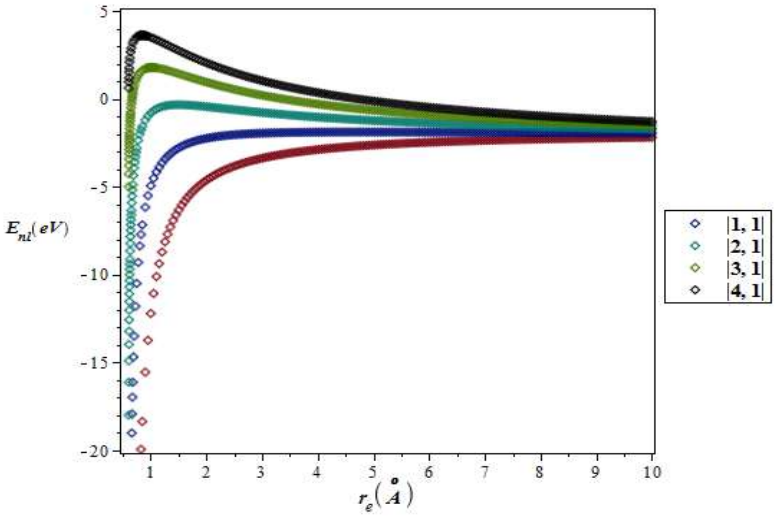

FIG. 4 Plot of energy eigenvalue spectrum against equilibrium bond length

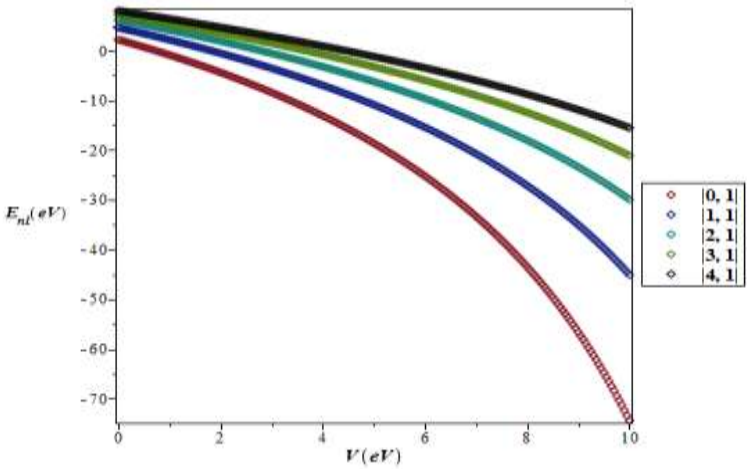

FIG. 5 Plot of energy eigenvalue spectrum against Coupling strength

7.0 Conclusion

In this study, the energy eigenvalues and corresponding normalized eigenfunctions for a linear combination of the modified Kratzer and generalized inverse quadratic Yukawa potentials were obtained using two distinct analytical approaches, namely the exact quantization rule method and the formula method. The thermodynamic properties of the system were subsequently evaluated through the partition function, enabling the determination of key observables such as the ro-vibrational mean energy, free energy, internal energy, entropy, and specific heat capacity.

Numerical results and graphical analyses were generated for selected diatomic molecules, including N_2, CO, NO, and CH, and compared with existing results reported in the literature. These comparisons were used to validate the accuracy of the present approach, while also providing insight into the behavior of the energy spectrum as a function of the quantum numbers (n) and (l), as well as the potential parameters.

In addition, the energy eigenvalues for the modified Kratzer plus generalized inverse quadratic Yukawa potential were computed for the same set of diatomic molecules to further investigate the influence of the combined potential on bound state systems. The results indicate that the energy spectrum increases with increasing values of both the principal quantum number (n) and the angular momentum quantum number (l), a behavior consistent with the expected characteristics of quantum bound states.

DECLARATIONS:

AVAILABILITY OF DATA AND MATERIALS

All data generated during this study are included in the references in the paper.

COMPETING INTERESTS

The authors declare that they have no competing interests.

Acknowledgement

Dr Etido P. Inyang gratefully acknowledges the National Open University of Nigeria for awarding the 2025 Senate Research Grant.

Funding: This study was supported by the National Open University of Nigeria through the 2025 Senate Research Grant (NOUN/SRG25/FASC/027).

Author contributions:

Etido P. Inyang: Conceived and designed the study, acquired, analyzed, and interpreted the data, and oversaw the review process. Jonathan E. Osang and Christopher C. Ekechukwu: Performed formal and computational analysis. Oyelami O. Abiodun, Olumuyiwa O. Akintola and Eddy S. William: Revised the manuscript for critical intellectual content and contributed to the general recommendations and data interpretation. All authors have read and approved the final manuscript.

REFERENCES

[1] E.S. William, E.P. Inyang, I.O. Akpan, J.A. Obu, A.N. Nwachukwu, and E.P. Inyang, *Indian Journal of Physics*, (2022). https://doi.org/10.1007/s12648-022-02308-0

[2] E.P. Inyang, N. Ali, R. Endut, N. Rusli, and S.A. Aljunid, *Indian Journal of Physics* (2024). https://doi.org/10.1007/s12648-024-03335-9

[3] E.S. William, S.C. Onye, A.N. Ikot, A.N. Nwachukwu, E.P. Inyang, I.B. Okon, I.O. Akpan, and B.I. Ita, *Journal of Theoretical and Applied Physics*, (2023). https://doi.org/10.30495/JTAP.172318
[4] E.S. William, I.B. Okon, O.O. Ekerenam, I.O. Akpan, B.I. Ita, E.P. Inyang, I.P. Etim, and I.F. Umoh, *International Journal of Quantum Chemistry*, (2022). https://doi.org/10.1002/qua.26925
[5] F. Ayedun, E.P. Inyang, E.A. Ibanga, and K.M. Lawal, *East Eur. J. Phys.*, 4 (2022), 87-98. https://doi.org/10.26565/2312-4334-2022-4-06
[6] E. Omugbe, O.E. Osafile, I.B. Okon, E.P. Inyang, E.S. William, and A. Jahanshir, *Few-Body Systems*, 63, 7 (2022).
[7] E.P. Inyang, E.O. Obisung, E.S. William, and I.B. Okon, *East European Journal of Physics*, 3 (2022), 114. https://doi.org/10.26565/2312-4334-2022-3-14
[8] E.S. William, J.A. Obu, I.O. Akpan, E.A. Thompson, and E.P. Inyang, *European Journal of Applied Physics*, 2 (2020), 28. http://dx.doi.org/10.24018/ejphysics.2020.2.6.28.
[9] E.S. William, E.P. Inyang, and E.A. Thompson, *Rev. Mex. Fis.*, 66 (2020), 730. https://doi.org/10.31349/RevMexFis.66.730
[10] E.P. Inyang, J. Ntibi, E.A. Ibanga, F. Ayedun, E.P. Inyang, and E.S. William, *AIP Conference Proceedings*, 2679 (2023), 030003. https://doi.org/10.1063/5.0112829
[11] E.P. Inyang, E.S. William, and J.A. Obu, *Rev. Mex. Fis.*, 67 (2021), 193. https://doi.org/10.31349/RevMexFis.67.193
[12] E.P. Inyang, E.P. Inyang, E.S. William, and E.E. Ibekwe, *Jord. J. Phys.*, 14 (2021), 345.
[13] C.O. Edet, S. Mahmoud, E.P. Inyang, N. Ali, S.A. Aljunid, R. Endut, A.N. Ikot, and M. Asjad, *Mathematics*, 10, (2022), 2824. https://doi.org/10.3390/math10152824
[14] E. S., Eyube, C. R. Makasson, E. Omugbe, C. A. Onate, E. P. Inyang, A. M. Tahir, & S. D. Najoji, *J. Mol.Model.*, *30*(12), (2024) 419. https://doi.org/10.1007/s00894-024-06208-4
[15] E. P. Inyang, E. P. Inyang, E. S. William, J. E. Ntibi, and E. A. Ibanga, *Bulgarian Journal of Physics*, 20 (2022), 1-11.
[16] E.P. Inyang, P.C. Iwuji, J.E. Ntibi, E. Omugbe, E.A. Ibanga, and E.S. William, *East European Journal of Physics*, 2 (2022), 51. https://doi.org/10.26565/2312-4334-2022-2-05
[17] E.P. Inyang, E.O. Obisung, J.A. Amajama, D.E. Bassey, E.S. William, and I.B. Okon, *Eurasian Physical Technical Journal*, 19(4(42)), (2022), 87. https://doi.org/10.31489/2022No4/78-87
[18] E.P. Inyang, Joseph E. Ntibi, Olumuyiwa O. Akintola, Efiong A. Ibanga, Funmilayo Ayedun, and Eddy S. William, *Communication in Physical Science*, 8(2), (2022), 244.
[19] E.P. Inyang, P.C. Iwuji, J.E. Ntibi, E.S. William, and E.A. Ibanga, *East European Journal of Physics*, 1 (2022), 11. https://doi.org/10.26565/2312-4334-2022-2-02
[20] E.P. Inyang, E.P. Inyang, J.E. Ntibi, and E.S. William, *Bulletin of Pure and Applied Sciences*, 40, 24 (2021), 10.5958/2320-3218.2021.0002.6
[21] E. Omugbe, *Asian Journal of Physics and Chemistry*, 26 (2020), 36.
[22] E. Omugbe, O.E. Osafile, E.P. Inyang, and A. Jahanshir, *Physica Scripta*, 96(12), 125408 (2021).
[23] E. Omugbe, O.E. Osafile, I.B. Okon, E.S. Eyube, E.P. Inyang, U.S. Okorie, A. Jahanshir, and C.A. Onate, *European Physical Journal D*, 76:72 (2022), 11.
[24] E.E. Ibekwe, J.B. Emah, E.P. Inyang, and A.O. Akpan, *Iran J. Sci. Technol Trans Sci*, (2022). https://doi.org/10.1007/s40995-022-01377-4
[25] A.N. Ikot, L.F. Obagboye, U.S. Okorie, E.P. Inyang, P.O. Amadi, and A. Abdel-Aty, *The European Physical Journal Plus*, 137 (2022), 1370. https://doi.org/10.1140/epjp/s13360-022-03590-x
[26] E.P. Inyang, N. Ali, R. Endut, N. Rusli, S.A. Aljunid, N.R. Ali, and M. Asjad, *East Eur. J. Phys.*, 1 (2024), 156–166. https://doi.org/10.26565/2312-4334-2024-1-13.

[27] S.M. Ikhdair and R. Sever, *J. Mol. Struct.-Theochem*, 855 (2008), 13.
[28] R.G. Newton, *Quantum Physics: A Text for Graduate Students*, Springer-Verlag, New York, (2002).
[29] E.P. Inyang, E.P. Inyang, I.O. Akpan, J.E. Ntibi, and E.S. William, *Canadian J. Phys.*, (2021). https://doi.org/10.1139/cjp-2020-0578
[30] Dong S.H., *Wave Equations in Higher Dimensions*, Dordrecht: Springer, (2011).
[31] Dong S.H., Morales D., and Gracia-Ravelo J., *Int. J. Phys.*, 16 (2007), 189.
[32] Ma Z.Q. and Xu B.W., *Europhys. Lett.*, 69 (2005), 685.
[33] E.P. Inyang, F.O. Faithpraise, J.Amajama, E.S. William, E.O. Obisung, and J.E. Ntibi, *East Eur. J. Phys.*, 1 (2023), 28. https://doi.org/10.26565/2312-4334-2023-1-03
[34] A. Kratzer, *Z. Phys.*, 3 (1920), 289.
[35] E.E. Ibekwe, U.S. Okorie, J.B. Emah, E.P. Inyang, S.A. Ekong, *Eur. Phys. J. Plus*, 87 (2021), 48.
[36] R.J. Le Roy and R.B. Bernstein, *J. Chem. Phys.*, 52 (1970), 3869.
[37] E.P. Inyang and E.O. Obisung, *East Eur. J. Phys.*, 3 (2022), 32. https://doi.org/10.26565/2312-4334-2022-3-04.
[38] H. Hassanabadi, H. Rahimov, and S. Zarrinkamar, *Adv. High Energy Phys.*, 458087 (2011), 1.
[39] S.M. Ikhdair, M. Hamzavi, and B.J. Falaye, *Appl. Math. Comput.*, 225 (2013), 775.
[40] M. Hamzavi, S.M. Ikhdair, and B.I. Ita, *Physica Scripta*, 85 (2012), 045009.
[41] S.M. Ikhdair, *Central Eur. J. Phys.*, 10 (2012), 361.
[42] S.J. Lee, H.H. Gan, E.D. Cooper, and S. Das Gupta, *Phys. Rev. C*, 40 (1989), 2585.
[43] E.P. Inyang, E.P. Inyang, J.E. Ntibi, E.E. Ibekwe, and E.S. William, *Ind. J. Phys.*, (2021). https://doi.org/10.1007/s12648-020-01933-x.
[44] C.O. Edet, P.O. Okoi, and S.O. Chima, *Rev. Bras. Ens. Fís.*, 42 (2020), e20190083.
[45] C.O. Edet, S.U. Okorie, A.T. Ngiangia, and A.N. Ikot, *Indian J. Phys.*, (2019), https://doi.org/10.1007/s12648-019-01477-9.
[46] O. Oluwadare and K. Oyewumi, *Chinese Phys. Lett.*, 34 (2017), 110301.
[47] E. P. Inyang, *Iranian Journal of Physics Research, 25*(3), (2025), 12031. https://doi.org/10.47176/ijpr.25.3.12031.
[48] E.P. Inyang, A.E.L. Aouami, N. Ali, R. Endut, N.R. Ali, and S.A. Aljunid, *Physics Open*, 2024, 100220. https://doi.org/10.1016/j.physo.2024.100220.
[49] E.P. Inyang, N. Ali, R. Endut, and S.A. Aljunid, *Eurasian Phys. Tech. J.*, 21 (2024), No. 1(47), 124–137. https://doi.org/10.31489/2024No1/124-137.
[50] C. Berkdemir, A. Berkdemir, and J. Han, *Chem. Phys. Lett.*, 417 (2006), 326–329.
[51] E.P. Inyang, E.S. William, J.A. Obu, B.I. Ita, E.P. Inyang, and I.O. Akpan, *Mol. Phys.*, e1956615 (2021). https://doi.org/10.1080/00268976.2021.1956615.
[52] O. Bayrak, I. Boztosun, and H. Cifti, *Int. J. Quant. Chem.*, 107 (2007), 540.
[53] S.H. Dong, *Wave Equations in Higher Dimensions*, Dordrecht: Springer (2011).
[54] M.E. Udoh, U.S. Okorie, M.I. Ngwueke, E.E. Ituen, and A.N. Ikot, *J. Mol. Model.*, 25 (2019), 1.
[55] R.L. Greene and C. Aldrich, *Phys. Rev. A*, 14 (1976), 2363.
[56] B.J. Falaye, S.M. Ikhdair, and H. Hamzavi, *Few-Body Syst.*, DOI: 10.1007/s00601-014-0937-9 (2014).
[57] M. Abramowitz and I.A. Stegun, *Handbook of Mathematical Functions with Formulas, Graphs and Mathematical Tables*, Dover, New York (1964).
[58] C. Berkdemir, A. Berkdemir, and J. Han, *Chem. Phys. Lett.*, 417 (2006), 326.
[59] C.A. Onate and J.O. Ojonubah, *J. Theor. Appl. Phys.*, 10 (2016), 21.

[60] C.A. Onate, M.C. Onyeaju, A.N. Ikot, and O. Ebomwonyi, *Eur. Phys. J. Plus*, 132 (2017), 462.
[61] E.P. Inyang, E.S. William, J.E. Ntibi, J.A. Obu, P.C. Iwuji, and E.P. Inyang, *Can. J. Phys.*, 100(10) (2022), 473. https://doi.org/10.1139/cjp-2022-003
[62] E.P. Inyang, A.N. Ikot, E.P. Inyang, I.O. Akpan, J.E. Ntibi, E. Omugbe, and E.S. William, *Results Phys.*, 105754 (2022). https://doi.org/10.1016/j.rinp.2022.105754.
[63] C.S. Jia, L.H. Zhang, and C.W. Wang, *Chem. Phys. Lett.*, 667 (2017), 211.
[64] M. Karakoc and I. Boztosun, *Int. J. Mod. Phys. E*, 15 (2006), 1253.
[65] G.B. Koksal, K. Bakir, and E. Gonul, *Phys. Scr.*, 73 (2006), 279.
[66] B. Chakrabarti and T.K. Das, *Phys. Lett. A*, 285 (2001), 11.
[67] F.J. Rogers, H.C. Graboske Jr., and D.J. Harwood, *Phys. Rev. A*, 1 (1970), 1577.
[68] E.P. Inyang, E.O. Obisung, P.C. Iwuji, J.E. Ntibi, J. Amajama, and E.S. William, , *J. Nig. Soc. Phys. Sci.*, 4 (2022), 884. https://doi.org/10.46481/jnsps.2022.884.
[69] E. P. Inyang, P. Okoi,, and I. Nwachukwu, *Eurasian Physical Technical Journal*, *22*(4), (2025), 101–116. https://doi.org/10.31489/2025N4/101-116
[70] E. P. Inyang, *Journal of Mathematical Chemistry*, *63*, (2025). 1732–1752. https://doi.org/10.1007/s10910-025-01738-5
[71] E. P. Inyang, *Journal of Theoretical Physics and Mathematics*, *3*(1), (2025) 1–10.
[72] E. P. Inyang, *Journal of Physics: Theories and Applications*, *9*(1), (2025). 23–36. https://doi.org/10.20961/jphystheor-appl.v9i1.97733

APPENDIX A

Some useful standard integrals used to evaluate the integrals in equation (5) are given below.

$$\int_{\tau_a}^{\tau_b} \frac{d\tau}{\sqrt{(\tau-\tau_a)(\tau_b-\tau)}} = \pi \tag{A1}$$

$$\int_{\tau_a}^{\tau_b} \frac{\tau d\tau}{\sqrt{(\tau-\tau_a)(\tau_b-\tau)}} = \frac{\pi}{2}(\tau_a+\tau_b) \tag{A2}$$

$$\int_{\tau_a}^{\tau_b} \frac{d\tau}{\tau\sqrt{(\tau-\tau_a)(\tau_b-\tau)}} = \frac{\pi}{\sqrt{\tau_a\tau_b}} \tag{A3}$$

APPENDIX B

In Cartesian coordinates, the 1D Schrödinger wave equation $\gamma(x)$ with a central potential $V(x)$ as given equation (2) is [68-72]

$$\frac{d^2\psi(x)}{dx^2} = -\frac{2\mu}{\hbar^2}\left[E-V(x)\right]\psi(x), \tag{B1}$$

and in 3D it is given by

$$\nabla^2\psi(r)+\frac{2\mu}{\hbar^2}\left[E-V(r)\right]\psi(r)=0, \tag{B2}$$

where $\nabla^2(r)$ is the Laplacian operator Cartesian coordinates.

To transform the one-dimensional Schrödinger equation into a three-dimensional one to accommodate the logarithmic derivative, the Laplacian, ∇^2 and the three-dimensional Schrödinger equation must be expressed in spherical polar coordinates. In spherical coordinates ∇^2 is given as

$$\nabla^2 = \frac{1}{r^2}\frac{\partial}{\partial r}\left(r^2\frac{\partial}{\partial r}\right)+\frac{1}{r^2\sin\theta}\frac{\partial}{\partial r}\left(\sin\theta\frac{\partial}{\partial\theta}\right)+\frac{1}{r^2\sin^2\theta}\frac{\partial^2}{\partial\varphi^2}. \tag{B3}$$

The three-dimensional form of the Schrödinger equation in spherical coordinates is written in the form $\psi(r,\theta,\varphi)$ and it is variable separable, i.e. it can be separated into its component as

$$\psi(r,\theta,\varphi)=\chi(r)\Theta(\theta)\phi(\varphi) \qquad \text{B4}$$

Substituting equations (3 and 4) into equation (2) yields

$$\frac{\Theta(\theta)\phi(\varphi)}{r^2}\frac{\partial}{\partial r}\left(r^2\frac{\partial\chi(r)}{\partial r}\right)+\frac{\chi(r)\phi(\varphi)}{r^2\sin\theta}\frac{\partial}{\partial\theta}\left(\sin\theta\frac{\partial\Theta(\theta)}{\partial\theta}\right)+\frac{\chi(r)\Theta(\theta)}{r^2\sin^2\theta}\frac{\partial^2\phi(\varphi)}{\partial\varphi^2} \qquad \text{B5}$$

$$+\frac{2\mu}{\hbar^2}\left[E-V(r)\right]\chi(r)\Theta(\theta)\phi(\varphi)=0$$

Dividing eq. (B5) by $\psi(r,\theta,\varphi)=\chi(r)\Theta(\theta)\phi(\varphi)$ and multiplying through by $r^2\sin^2\theta$ yields

$$\frac{\sin^2\theta}{\chi(r)}\frac{\partial}{\partial r}\left(r^2\frac{\partial\chi(r)}{\partial r}\right)+\frac{\sin\theta}{\Theta(\theta)}\frac{\partial}{\partial\theta}\left(\sin\theta\frac{\partial\Theta(\theta)}{\partial\theta}\right)+\frac{2\mu r^2\sin^2\theta}{\hbar^2}\left[E-V(r)\right]=-\frac{1}{\phi(\varphi)}\frac{\partial^2\phi(\varphi)}{\partial\varphi^2} \qquad \text{B6}$$

The RHS and the LHS of equation (B6) are both independent and so they are equal to the same constant $m_\ell^{\,2}$, say. That is

$$\frac{1}{\phi(\varphi)}\frac{\partial^2\phi(\varphi)}{\partial\varphi^2}=-m_\ell^{\,2} \qquad \text{B7}$$

where m_ℓ is the magnetic quantum number.

Substituting equation (B7) into equation (B6) and dividing through by $\sin^2\theta$ gives

$$\frac{1}{\chi(r)}\frac{\partial}{\partial r}\left(r^2\frac{\partial\chi(r)}{\partial r}\right)+\frac{2\mu r^2}{\hbar^2}\left[E-V(r)\right]+\frac{1}{\sin\theta}\frac{1}{\Theta(\theta)}\frac{\partial}{\partial\theta}\left(\sin\theta\frac{\partial\Theta(\theta)}{\partial\theta}\right)-\frac{m_\ell^{\,2}}{\sin^2\theta}=0 \qquad \text{B8}$$

The radial and angular parts of equation (B8) are linearly independent and therefore are equal to a constant, $l(l+1)$ say. That is,

$$\frac{1}{\chi(r)}\frac{\partial}{\partial r}\left(r^2\frac{\partial\chi(r)}{\partial r}\right)+\frac{2\mu r^2}{\hbar^2}\left[E-V(r)\right]=l(l+1) \qquad \text{B9}$$

and

$$\frac{1}{\sin\theta}\frac{1}{\Theta(\theta)}\frac{\partial}{\partial\theta}\left(\sin\theta\frac{\partial\Theta(\theta)}{\partial\theta}\right)-\frac{m_\ell^{\,2}}{\sin^2\theta}=-l(l+1) \qquad \text{B10}$$

Equation (B9) is the radial part of the Schrödinger equation (which is the equation of interest). Solving and re-writing it as an ordinary differential equation yield

$$r^2\frac{d^2\chi(r)}{dr^2}+2r\frac{d\chi(r)}{dr}+\frac{2\mu r^2}{\hbar^2}\left[E-V(r)-\frac{\hbar^2}{2\mu r^2}l(l+1)\right]\chi(r)=0\,. \qquad \text{B11}$$

Multiplying equation (11) by r^2 yields

$$\frac{d^2\chi(r)}{dr^2}+\frac{2}{r}\frac{d\chi(r)}{dr}+\frac{2\mu}{\hbar^2}\left[E-V(r)-\frac{\hbar^2}{2\mu r^2}l(l+1)\right]\chi(r)=0 \qquad \text{B12}$$

To solve the above equation, we make use of a trial wave function that obeys the cusp condition (or Kato's theorem). One of such function is of the form:

$\chi(r)=r^{-1}R(r)$.

and
$$\frac{d}{dr}\chi(r) = -r^{-2}R(r) + r^{-1}\frac{d}{dr}R(r)$$
$$\frac{d^2}{dr^2}\chi(r) = 2r^{-3}R(r) - r^{-2}\frac{d}{dr}R(r) + r^{-1}\frac{d^2}{dr^2}R(r) - r^{-2}R(r) \quad \text{B13}$$

Substituting equation (B13) into equation (B12) and simplifying gives

$$\frac{d^2R(r)}{dr^2} = -\frac{2\mu}{\hbar^2}\left[E - V_{eff}(r)\right]R(r), \quad \text{B14}$$

as given in equation (7) of the article.

Appendix C

The second order differential equation can be written in the form

$$\psi''(s) + \frac{(k_1 - k_2 s)}{s(1-k_3 s)}\psi'(s) + \frac{\left(As^2 + Bs + C\right)}{s^2(1-k_3 s)^2}\psi(s) = 0 \quad \text{C1}$$

The wave function of the differential equation above can be determined from the formula

$$\psi(s) = N_n s^{k_4}(1-k_3 s)^{k_5}\,{}_2F_1\left(-n, n + 2(k_4 + k_5) + \frac{k_2}{k_3} - 1; 2k_4 + k_1, k_3 s\right) \quad \text{C2}$$

where the parameters are defined as

$$k_4 = \frac{(1-k_1) + \sqrt{(1-k_1)^2 - 4C}}{2} \quad \text{C3}$$

and

$$k_5 = \frac{1}{2} + \frac{k_1}{2} - \frac{k_2}{2k_3} + \sqrt{\left[\frac{1}{2} + \frac{k_1}{2} - \frac{k_2}{2k_3}\right]^2 - \left[\frac{A}{k_3^2} + \frac{B}{k_3} + C\right]} \quad \text{C4}$$